

The potential contribution of soil moisture to fog formation in the Namib Desert

Bishwodeep Adhikari and Lixin Wang*

Department of Earth Sciences, Indiana University-Purdue University Indianapolis (IUPUI),
Indianapolis, IN 46202 USA

* Corresponding author:

Lixin Wang (lxwang@iupui.edu)

Department of Earth Sciences

Indiana University-Purdue University Indianapolis

Indianapolis, IN 46202, USA

Office phone number: 1-317-274-7764

Fax: 1-317-274-7966

This is the author's manuscript of the article published in final edited form as:

Adhikari, B., & Wang, L. (2020). The potential contribution of soil moisture to fog formation in the Namib Desert. *Journal of Hydrology*, 591, 125326. <https://doi.org/10.1016/j.jhydrol.2020.125326>

Abstract

Fog is considered as an important source of water in many drylands, and the knowledge of possible sources of its formation is essential to make future predictions. Prior studies have suggested the presence of locally generated fog in drylands; however, its formation mechanism remains unclear. There have been studies on the effects of fog on soil moisture dynamics. On the contrary, no research has yet been conducted to understand the potential contribution of soil moisture to fog formation. This study, therefore, for the first time intends to examine such possibility in a fog-dominated dryland ecosystem, the Namib Desert. The study was conducted at two sites representing two different land forms (sand dunes and gravel plains) in the Namib Desert. We first examined evidence of fog formation through water vapor movement using field observations, and then simulated water vapor transport using HYDRUS-1D model. In the first part of the study, soil moisture, soil temperature and air temperature data were analyzed, and the relationships between these variables were taken as one of the key indicators for the linkage between soil water and fog formation. The analysis showed that increase in soil moisture generally corresponded to similar increase in air or soil temperature near the soil surface, which implied that variation in soil moisture might be the result of water vapor movement (evaporated soil moisture) from lower depths to the soil surface. In the second part of the study, surface fluxes of water vapor were simulated using the HYDRUS-1D model to explore whether the available surface flux was sufficient to support fog formation. The surface flux and cumulative evaporation obtained from the model showed positive surface fluxes of water vapor. Based on the field observations and the HYDRUS-1D model results, it can be concluded that water vapor from soil layers is transported through the vadose zone to the surface and this water vapor likely contributes to the fog formation in fog-dominated drylands, like the Namib Desert.

Keywords: ecohydrology, drylands, fog, hydrological model, HYDRUS-1D, Namib Desert, soil moisture

1. Introduction

Drylands are regions where precipitation is comparatively less than potential evapotranspiration. The aridity index (AI), quantitatively defined as the ratio of precipitation to potential evapotranspiration, must be less than 0.65 for an area to be considered as drylands. Drylands can be classified using this aridity index into four sub-types: dry sub-humid lands, semi-arid lands, arid lands, and hyper-arid lands (Adeel et al., 2005; Wang et al., 2012). Drylands cover approximately 40% of the land surface and support more than 2 billion population worldwide (Wang et al., 2012).

Since water resources are severely limited in drylands, water availability poses the primary control over biological processes (Wang et al., 2010; Yu and D'Odorico, 2015). Fog, although in small amount, play an important supporting role in supplying water that is essential to maintain ecological functions in drylands (Wang et al., 2017). In arid drylands, where rainfall is sparse, fog can be the most important form of water input which could be utilized for the dryland ecosystem to increase productivity (Kaseke et al., 2017; Qiao et al., 2020). It can also constitute a major portion of the overall hydrological input especially in some of the coastal areas which often receive very little or no rainfall in a year (Dawson, 1998).

In general, there are seven types of fog, four of which are based on process and place of formation (radiation fog, sea fog, steam fog and advection fog), and the remaining three are designated based on their place of occurrence irrespective of the process of their formation (coastal fog, valley fog and mountain fog) (Eugster, 2008). Out of these seven different types of fog, most

studies have focused on two types, namely (i) radiation fog, which is formed mainly by a cooling mechanism, especially nocturnal cooling over the continental surface, and (ii) advection fog, which is formed because of the humidification near coastal areas or over the sea (Bergot and Guedalia, 1994).

Even though fog provides significant amount of water for dryland environments (Runyan et al., 2019), these are the least studied components of the hydrological cycle (Wang et al., 2017). Having multiple origins, fog in drylands can originate from recycling of groundwater via evapotranspiration and redistribution of water vapor in the upper soil layers. More than 50% of the total fog events in the Namib Desert were found to be non-ocean-derived during their study period (Kaseke et al., 2017). This highlights the importance of studies to determine the quantity and origin of fog in dryland ecosystems where rainfall is expected to decline due to climate change in coming years (Lu et al., 2016).

Soil moisture is considered as a critical component of Earth system and plays an important role in land-atmosphere interactions (Eltahir, 1998). It can be used to understand the relationship of climate, soil and vegetation in dryland ecosystems (Fang et al., 2016; Li et al., 2016). In water-limited dryland ecosystems, various eco-hydrological processes are dependent on soil water availability (Wang et al., 2009; Miller et al., 2012; Wei et al., 2019). Many factors like precipitation, evaporation, liquid water and water vapor flow influence soil moisture near the surface in drylands, and most of these factors are strongly connected. In the Namib Desert, the first millimeters of surface soil might receive enough soil moisture from fog droplets and dew formation (Li et al., 2016, Wang et al., 2019). Since soil water content near the soil surface in drylands is often extremely low, water vapor transport plays a critical role in the overall water flux and availability (D'Odorico and Porporato, 2006; Saito et al., 2006; Yin et al., 2019).

The movement of soil moisture and heat are coupled. The simultaneous movement of heat, liquid water and water vapor at the land-atmosphere interface is significant for a range of biological phenomena, as well as water and energy balance of terrestrial ecosystems (Bittelli et al., 2008; Cahill and Parlange, 1998; Saito et al., 2006). The total heat flux of soil is a result of simple conduction as well as the movement of water in both the liquid and vapor states. The net soil moisture movement between any two locations can be mainly attributed to the movement of moisture in soil from one location to another caused by evaporation and subsequent re-condensation. During this process of evaporation and re-condensation, a significant amount of energy is transported by the water vapor since water has high latent energy of vaporization (Cahill and Parlange, 1998; Saito et al., 2006).

Fog and soil moisture impact each other. Fog increases soil moisture, and sometimes fog infiltrates further down to recharge groundwater systems (Ingraham and Matthews, 1990). At the same time, soil water could contribute to fog formation. For example, using oxygen and hydrogen isotopes, a recent study showed that groundwater is a source of radiation fog in the Namib Desert (Kaseke et al., 2017). One possible process is through soil water evaporation and subsequent re-condensation. Previous studies have demonstrated that soil water can be transported from one location to another by evaporation and re-condensation (Bittelli et al. 2008; Cahill and Parlange 1998; Saito et al., 2006; Sakai et al., 2011). Furthermore, the transported soil water to the surface can be evaporated from the soil surface into atmosphere contributing to the formation of fog.

Past studies have explored the impact of fog to groundwater recharge or soil moisture content (Ingraham and Matthews, 1988, 1990; Li et al., 2018; Liu et al., 2005; Prada et al., 2010; Sawaske and Freyberg, 2015). Furthermore, prior studies have suggested the prevalence of radiation fog in addition to the advection fog in the Namib Desert (Kaseke et al., 2018). These

studies identified groundwater and soil moisture as possible origins for the radiation fog in the Namib Desert, but transport and formation mechanisms still remain unclear. This research hence for the first time aims to investigate the contribution of soil moisture to the formation of fog in the Namib Desert. The hypothesis of the study is that soil moisture contributes to the fog formation in the fog-dominated dryland, Namib Desert, through the process of continuous evaporation and subsequent condensation in sub-soil. To test this hypothesis, this research examined the relationships between volumetric soil water content, soil and air temperature, and fog occurrence in the study area. In addition, a hydrological model (HYDRUS-1D) was applied to simulate water vapor transport in the vadose zone to further evaluate the hypothesis.

2. Materials and Methods

2.1 Site description

The Namib Desert was chosen for the study because it is a fog-dominated dryland. It is located in the coastal area of Namibia and extends from the Olifants River in South Africa to Carunjamba River in Angola, and has an overall stretch of 1,900 km along the coast of the Atlantic Ocean (Li et al., 2016). There is a wide distribution of precipitation in the Namib Desert with an annual average of 5-18 mm in the central Namib Desert (Li et al., 2016).

Two land forms, the gravel plains and the sand dunes at Gobabeb located in the Namib Desert, were selected since they share similar meteorological conditions but different soil textures. The study sites were located within the vicinity of the Gobabeb Research and Training Centre (lat. -23.55°, long. 15.04°, and elv. 405 m.a.s.l.), which is in the Central Namib Desert and about 60 km inland from the Atlantic Ocean (Figure 1). The Gobabeb Centre is surrounded by three main land forms: gravel plains to the north and east (91% sand, 0.6% clay and 8.4% silt), sand dune sea

to the west and south (74.8% sand, 5.5% clay and 19.7% silt), and the ephemeral Kuiseb River (91.5% sand, 2.1% clay, 6.4% silt) to the south of the Centre which separates the gravel plains and sand dune sea (Kaseke et al., 2017). The climate at Gobabeb is hyper-arid with extremely infrequent precipitation events and a mean annual precipitation of 27 mm. The mean monthly temperature at Gobabeb ranges from 17 to 24.2°C, and has an average relative humidity of around 50%, with 94 mean annual foggy days (Eckardt et al., 2013; Li et al., 2018).

2.2 Data collection

The volumetric water content and soil temperature data used in the study were collected from two sites at Gobabeb in the Namib Desert; the gravel plains and the sand dunes. The volumetric water content and soil temperature data were measured hourly at both sites using the CS655 Water Content Reflectometer (Campbell Scientific, Inc. Logan, Utah, USA). The soil probes were located at an approximate depth of 4 cm at both sites. These soil moisture probes were installed horizontally at the sites and can detect volumetric water content from 0 to 100% (with M4 command) with a high precision (<0.05%). The daily precipitation data were collected using the tipping-bucket setting at the gravel plains and the same data were used for the sand dunes as well because of their close proximity. Other meteorological data such as air temperature and fog were obtained from weather and Fognet stations, which are part of the Southern African Science Service Centre from Climate Change and Adaptive Land Management (SASSCAL). For the gravel plains, volumetric water content and soil temperature data from December 29, 2013 to June 24, 2018, and for the sand dunes, data from August 5, 2015 to May 22, 2018 were used in the analysis.

Furthermore, soil moisture and soil temperature data used by Entekhabi et al. (2001) to evaluate relationship between surface temperature and soil moisture in southern Africa was retrieved and digitized to compare results of their study to those of the present research. The study

by Entekhabi et al. (2001) was used to compare the results since the site considered in their study had a semi-arid climate and received a higher amount of rainfall as compared to the present research. In addition, that study represented general relationship between soil moisture and soil temperature, which would exist in most of the places with wetter climatic conditions.

2.3 Analysis of field data

Hourly volumetric water content, soil temperature, precipitation and fog data were used to obtain the daily values for analysis. In order to demonstrate the relationship of volumetric water content with soil and air temperature, simple scatter plots and box plots were used. Since relationships were found between volumetric soil water content and different variables such as soil temperature, air temperature, fog and precipitation, data were analyzed to determine how the change in volumetric water content can be explained by change in different variables. The statistical relationships between daily air/soil temperature and volumetric water content were tested using Spearman correlation coefficients. The soil and air temperature were divided into distinct 5°C bins for demonstrating the relationship with volumetric water content. The near surface soil temperature and air temperature were used for this study to further examine if the soil temperature follows the air temperature trend. Fog and precipitation data were used to understand how the volumetric soil water content responds to their occurrences or vice versa. The data were analyzed for two periods: (i) all the available data and (ii) data from August 19, 2015 to November 6, 2015 during which there was no rainfall event, in order to examine whether the relationship varies when rainfall events are considered and during periods with no rainfall events. The 80 non-rainfall days (August 19, 2015 to November 6, 2015) were chosen mainly because there were no data missing within that period, there were several fog events during that period, and this period was the one previously used by Li et al. (2018) to examine the effects of fog on soil moisture

dynamics in the Namib Desert. Furthermore, the statistical analysis of data was done based on hydrologic year (October to September) since rainfall events at Gobabeb are very rare, but if these events occur, they are mostly concentrated between October and April (Lu et al., 2016). The rainfall seasonal distribution at the study sites is similar to Windhoek where the rainfall is very seasonal and concentrated within the above mentioned months (Kaseke et al., 2018).

2.4 HYDRUS modeling

2.4.1 Model description

HYDRUS-1D model is often used for the simulation of one-dimensional water flow, heat movement and solute transport in variably saturated porous media (Šimůnek et al., 2013). In the present study, version 4.17 of this model was used for the simulation of water vapor transport from groundwater and soil moisture to the soil surface. The basic equation HYDRUS-1D model uses for the water flow is Richards equation.

$$\frac{\partial \theta}{\partial t} = \frac{\partial}{\partial x} \left[K \left(\frac{\partial h}{\partial x} + \cos \alpha \right) \right] - S, \quad (1)$$

where $\theta(h)$ is the volumetric water content, t is time, x is the spatial coordinate considering upward direction as positive, $K(h)$ is the unsaturated hydraulic conductivity, h is the water pressure head, α is the angle between the flow direction and vertical axis, and S is the sink term (see HYDRUS-1D User Manual by Šimůnek et al. (2013)).

However, since Richards equation considers only liquid flow and ignores vapor flow, HYDRUS-1D model uses the following non-isothermal liquid and vapor flow equation (Saito et al., 2006) for the water vapor transport modeling.

$$\frac{\partial \theta_T(h)}{\partial t} = \frac{\partial}{\partial x} \left[(K + K_{vh}) \left(\frac{\partial h}{\partial x} + \cos \alpha \right) + (K_{LT} + K_{vT}) \frac{\partial T}{\partial x} \right] - S(h), \quad (2)$$

where θ_T is the total volumetric water content, T is temperature in Kelvin, K is the isothermal hydraulic conductivity of the liquid phase, K_{LT} is the thermal hydraulic conductivity of

the liquid phase, K_{vh} is the isothermal vapor hydraulic conductivity, and K_{vT} is the thermal vapor hydraulic conductivity (see HYDRUS-1D User Manual by Šimůnek et al. (2013)).

2.4.2 Model setup

HYDRUS-1D model was used to simulate water vapor flow and heat transport in the vertical direction. Horizontal water transport was not considered. The soil column was considered to be homogeneous along the depth (e.g., soil was regarded as a single layer for the simulation). The hydraulic sub-model within HYDRUS-1D used for this study was Van Genuchten-Mualem model (Van Genuchten, 1980). Since the simulated study sites have very low vegetation cover, plant transpiration was neglected and only evaporation was considered for this study. The inverse solution option available in HYDRUS-1D was used in order to optimize the soil hydraulic parameters, alpha (a fitting parameter) and n (pore-size distribution index), which are the coefficients of soil water retention function (see HYDRUS-1D User Manual, Šimůnek et al. (2013)).

The simulations were validated using the measured soil temperature and volumetric soil water content at a depth of 4 cm at the sand dunes and the gravel plains. The validation period was considered after a certain duration of the model run in order to provide sufficient model spin-up time. The validation was done after 40 days at the sand dunes site since only 93 days were run in the model, and the simulation results was obtained for 53 days. The model spin-up period provided at the gravel plains was approximately 50% of the overall time period (129 days) selected for the model run and 65 days were used for the results. The model was run for the rainless period to examine if the soil moisture will have sufficient surface flux and evaporation for the formation of fog at the sites. The actual surface flux obtained from the model inform what actually happens at the surface, whether the soil water evaporates or infiltrates (e.g., fraction of water moves

downward). The higher amount of evaporation obtained from the model would suggest more soil water transported to the atmosphere, while higher amount of infiltration would suggest less soil water transported to the atmosphere.

2.4.3 Soil hydraulic and heat transport parameters

The soil hydraulic parameters required for the simulation of HYDRUS-1D are residual water content (Q_r), saturated water content (Q_s), saturated hydraulic conductivity (K_s), parameter α in the soil water retention function (*Alpha*), parameter n in the soil water retention function (n), and tortuosity parameter in the conductivity function (l). All these parameters except *Alpha* and n were kept constant throughout the simulation and were obtained by the neural network prediction function (Rosetta Lite v. 1.1, (Schaap et al., 2001)) available in the HYDRUS-1D model by providing the percentage of sand, silt and clay of the soils. For this study, the percentage of sand, silt and clay at the sand dunes were 74.8, 19.7 and 5.5%, and were 91, 8.4 and 0.6% at the gravel plains, respectively. The parameter *Alpha* and n were optimized during the calibration by inverse modeling (available in HYDRUS-1D model) of daily observed volumetric water contents of the soil at selected depths and locations. The soil hydraulic parameters used for the study are presented in Table 1.

The heat transport parameters for the model are volume fraction of solid phase and organic matter, longitudinal thermal dispersivity, coefficient b_1 , b_2 and b_3 for thermal conductivity function, and volumetric heat capacities of solid phase (C_n), organic matter (C_o) and liquid phase (C_w). The default values of coefficients for thermal conductivity function and volumetric heat capacities as provided by the HYDRUS-1D model are used for both sites, and the thermal conductivity equation provided by Chung and Horton (1987) was used for the heat transport process. The heat transport parameters used in the study are presented in Table 2.

2.4.4 Initial and boundary conditions

In order to solve the Richards equation for water flow, the initial distribution of pressure head or water content within the flow domain is required. In this study, the initial condition is provided in terms of water content as:

$$\theta(x, t) = \theta_i(x) \quad , \quad t = t_0 \quad (2.3)$$

where $\theta_i[L]$ is defined as a water content function of x , and t_0 is the time when the simulation starts (see HYDRUS-1D User Manual, Šimůnek et al. (2013)). Since the daily variation of water content was used for the simulation in this study, the water content and temperature values prior to the day selected as first day of simulation were set as initial quantities.

The atmospheric boundary conditions with surface layer were selected for the water flow at the upper boundary. Precipitation, potential evapotranspiration, minimum allowed pressure head at the soil surface that facilitate evaporation, and time-dependent temperature of the soil surface were supplied into the model at a daily temporal resolution as time variable boundary conditions at upper boundary. The average evaporation of 0.65 mm/day at the gravel plains (Li et al., 2018) was used for the simulation period at both sites because of their close proximity, and the plant transpiration was neglected since there were very low vegetation cover around the sites. At the lower boundary, variable flux condition was used since soil moisture will change with time due to evaporation, and flux will not be temporally constant. The time dependent temperature of soil at the surface and lower boundary was considered as the boundary conditions for the heat transport process.

3. Results

3.1 Statistics of soil water content, fog and temperature

The mean volumetric water content for the entire study period at the sand dunes and the gravel plains were found to be 0.771% and 2.105%, respectively (Table 3). The Kurtosis (K-value) and the skewness of the mean volumetric water content for the entire study period at the sand dunes was 34.82 and 4.95, respectively (Table 3). For the gravel plains, the K-value was 18.52 with the skewness of 3.90 during the entire study period (Table 3). The average volumetric water content at the sand dunes and the gravel plains for the 80 non-rainfall days from August 19, 2015 to November 06, 2015 was found to be 0.639% and 1.499%, respectively (Table 3). For the 80 non-rainfall period, the K-value and skewness were 0.47 and -0.54, respectively at the sand dunes, and were 1.20 and 0.73, respectively at the gravel plains (Table 3). These values (Table 3) and QQ-plot (see Figure 1 and 2 in supplementary materials) indicated that the volumetric water content was normally distributed around their respective means for the 80 non-rainfall days while it deviated from normality for the entire study period at both sites. The volumetric water content at both sites seemed to have nearly daily fluctuations with few distinct peaks within the study period (Figure 2). There were few rainfall events but whenever there was a rainfall event, the volumetric water content reached a peak which descended gradually over time. Sometimes during the descending phases, there were various fog events (Figure 2).

The average annual rainfall at the study site was only 24.9 ± 29.13 mm based on five hydrologic years. The rainfall in the 2017-2018 hydrologic year was extremely high (75.4 mm), while it remained below 25 mm for the remaining four hydrologic years. There were only 18 rainfall days during the five hydrologic years considered in the study. The average annual fog at the site was 132.79 mm with 184 fog days during three hydrologic years (two years' fog data not

available, Table 4). There were 24 fog days during the 80 non-rainfall period from August 19, 2015 to November 06, 2015. The average water content was $2.13 \pm 0.5\%$ for the five hydrologic years at the gravel plains and was $0.76 \pm 0.2\%$ for four hydrologic years at the sand dunes (one-year data not available, Table 4). When the atypical hydrologic year (2017-2018) with very high rainfall was removed, the average water content was $1.94 \pm 0.1\%$ for the gravel plains and was $0.66 \pm 0.1\%$ for the sand dunes (Table 4).

The mean soil temperature and air temperature at both sites displayed similar trends. At the sand dunes, the mean soil temperature during the entire study period was $24.09\text{ }^{\circ}\text{C}$, and was $25.30\text{ }^{\circ}\text{C}$ for the 80 non-rainfall period. Similarly, at the gravel plains, the mean soil temperature was $25.78\text{ }^{\circ}\text{C}$ for the entire study period and $23.48\text{ }^{\circ}\text{C}$ for the 80 non-rainfall period. The soil temperature varied from $16.09\text{ }^{\circ}\text{C}$ to $39.73\text{ }^{\circ}\text{C}$ for the entire study period and from $16.66\text{ }^{\circ}\text{C}$ to $32.38\text{ }^{\circ}\text{C}$ for the 80 non-rainfall period at the sand dunes, while it varied from $14.33\text{ }^{\circ}\text{C}$ to $37.41\text{ }^{\circ}\text{C}$ for the entire study period and from $16.07\text{ }^{\circ}\text{C}$ to $31.09\text{ }^{\circ}\text{C}$ for the 80 non-rainfall period at the gravel plains. Similarly, the air temperature ranged from $9.47\text{ }^{\circ}\text{C}$ to $33.63\text{ }^{\circ}\text{C}$ for the entire study period at the sand dunes and from $9.41\text{ }^{\circ}\text{C}$ to $33.63\text{ }^{\circ}\text{C}$ at the gravel plains, and from $11.84\text{ }^{\circ}\text{C}$ to $27.46\text{ }^{\circ}\text{C}$ for the 80 non-rainfall period at both sites.

3.2 Relationship between fog, volumetric soil water content and temperature

Soil temperature increased with increase in air temperature, and vice versa (Figure 2). The soil temperature was generally found to be higher than the air temperature. The analysis of soil temperature and volumetric water content at the sand dunes showed an increase in soil water content with increase in soil temperature (Figure 4 and Figure 5). The results were similar between the entire study period and during the 80 non-rainfall period (Figure 4 and Figure 5). Despite the greater number of outliers when the overall study period was considered (as compared to the 80

non-rainfall days), the relationship was not substantially affected. Likewise, the relationship between these variables showed similar characteristics at the gravel plains with an exception for soil temperatures below 15°C, i.e., the water content at soil temperature less than 15 °C was slightly higher as compared to the higher soil temperature groups. The relationship of water content with soil temperature was more pronounced and stronger at the sand dunes as compared to the gravel plains. In addition, the Spearman correlation coefficients (Table 3) also showed that there was a positive correlation between soil temperature and water content.

Similarly, the relationship of volumetric soil water content with air temperature was analyzed separately at both sites. At the sand dunes, this displayed a parallel pattern to the soil temperature and water content relationship. However, at the gravel plains, the relationship of soil water content was more noticeable with the air temperature as compared to the soil temperature. The outliers in the case of air temperature were more in the entire period than in the non-rainfall days, similar to the soil temperature and water content relationship. Soil water content increased with the increase in air temperature for the entire study period as well as the 80 non-rainfall days at both sites. Overall, the volumetric soil water content increased with increase in soil and air temperature at both sites, regardless whether the entire study period with rainfall events or the 80 rainless days were considered (Figure 4 and Figure 5).

Whenever there was a fog or rainfall event, the volumetric water content increased and reached a peak (Figure 2). However, it was also evident that as the volumetric water content declined, there were quite a few occurrences of fog events (Figure 2).

3.3 HYDRUS-1D Modeling

The HYDRUS-1D model was used to simulate the water vapor fluxes by comparing the volumetric soil water content as well as soil temperature available at the sites with model output.

At the sand dunes, the model was run from August 6, 2015 to November 6, 2015 with data on August 5, 2015 provided as the initial conditions. Even though the model was run from August 6, 2015, the water content obtained from the model were compared with the observed values after 40 days (approximately 43% of the simulation period) to allow a model spin up period. The model-data comparison result at the sand dunes site for soil water content was modest ($R^2=0.36$); the predicted water content values were similar except for the higher observed values of soil water content around October 6, 2015 (Figure 6). However, there was a very good fit between the simulated and observed soil temperature ($R^2=0.99$) (Figure 7). The mean observed volumetric soil water content for the validation period was 0.6639% and the average water content obtained from the model was 0.6641%. The cumulative actual surface flux (i.e., aggregated value of what actually happens in the surface; evaporation or the infiltration) obtained from the model was 0.304 mm (Figure 8). The cumulative infiltration was computed to be 0.184 mm at the end of the simulation period, while the cumulative evaporation was 0.714 mm, which is almost four times the cumulative infiltration.

Similarly, the model was run from July 1, 2015 to November 6, 2015 at the gravel plains site. The model output was compared with observations after approximately 50% of the simulation period as model spin-up period. The R^2 value for the simulation of soil water content was only 0.13 even though the simulated water content values were comparable (Figure 6). The average observed water content for the calibrated period was 1.482% and the average water content obtained from the model was 1.500%. The modeled water content at the gravel plains had declining slope and did not match the increased water content after October 21, 2015 similar to the sand dunes, hence a lower R^2 value. The simulation of soil temperature nevertheless showed almost a perfect fit similar to the sand dunes site ($R^2=0.99$) (Figure 7). The simulation at the gravel plains

was run for 129 days, and the cumulative actual surface water vapor flux obtained from the model was 8.968 mm (Figure 8). Unlike at the sand dunes, the gravel plains had total evaporation of 8.994 mm which is approximately 1430 times the infiltration (0.0063 mm).

4. Discussion

4.1 Field observations

It is known that the soil water content increases with rainfall and fog events (Li et al., 2016; Li et al., 2018). The occurrence of fog events during the decline of the soil water content (Figure 2 and Figure 3) when there were no rainfall events suggested the possibility of either advection or radiation fog (locally generated fog) formation at the site. However, these fog events are thought to be more radiative rather than advective. Kaseke et al. (2017) revealed that there are comparable radiation fog and advection fog in the fog zone of the Namib Desert for the study year, and more than half of the overall fog events during the study period are not sourced from the ocean. For a fog to be locally-generated, there should be a water source and since the study sites do not have permanent water source except the ephemeral Kuiseb river, the only possible sources are soil moisture and groundwater at the sites. However, soil moisture data were unavailable at the site with groundwater and hence only the soil moisture contribution was considered for this study.

The relationship between temperature and soil moisture was evaluated to examine the possibility of water vapor movement in this arid environment. In general, there is a positive relationship between soil temperature and soil moisture at both sites (Figure 4 and Figure 5). The relationship between air temperature and soil moisture was similar to the relationship between soil temperature and soil moisture, eliminating the possibility of biased results due to same sensor measuring soil moisture and soil temperature. The temperatures were found to be directly proportional to each other (Figure 2). There were outliers seen in the analysis of the soil

temperature and soil moisture during the overall study period (Figure 4 and Figure 5), which may be attributed to the rainfall events causing substantial change in soil water content over a short period of time. The small number of outliers seen during the analysis of 80 non-rainfall days may further justify the argument. The soil water content increased with increase in soil temperature at both sites (Figure 4 and Figure 5). A slight exception was seen in this relationship at the gravel plains, where at the lower soil temperature groups, the water content seemed to be a little higher than the following higher temperature groups. Similarly, even though the overall relationship of water content with the soil temperature appeared increasing at the sand dunes, the water content at the lower soil temperature groups was slightly higher than the following soil temperature group, as it was at the gravel plains. The positive relationship between soil water and soil temperature may be due to the process of condensation during the transport of water vapor originated from evaporated soil moisture from a certain depth. During this process, the transported water vapor condenses and adds up moisture to the soil. Condensation also increases soil temperature through the release of latent heat. Because the soil temperature and air temperature followed a similar pattern, it can be deduced that the soil water content would change with soil temperature in a similar way as it does with air temperature.

It is worth noting that the relationship between soil moisture and soil temperature observed in this study contrasts with the one presented by Entekhabi et al. (2001), where it is stated that the water content decreases when there is increase in the near surface soil temperature. The study was done in the Skukuza core site located in Kruger National Park, South Africa, which had an average annual rainfall of 546 mm. However, the setting considered in our study is entirely different than in Entekhabi et al. (2001). The site considered in our study, Gobabeb is extremely dry with average annual precipitation of only 24.9 mm. While the annual average rainfall was only around 12.3 mm

until 2017, the average raised up to 24.9 mm because of heavy rainfall event in April (36.1 mm) and May (30.8 mm) of 2018 (even though the data was available only until June 24, 2018). Generally, there would be a negative relationship between soil temperature and soil moisture in most of the places as seen in the study by Entekhabi et al. (2001). However, based on this study, it suggests that the drier the environment the stronger positive relationship between the soil temperature and soil moisture. Water from soil moisture and shallow groundwater may evaporate easily in a hot and dry environment, hence the strong positive relationship between soil temperature and soil moisture in such an environment, like the Namib Desert. This brings up the fact that the relationship between soil temperature and water content can be different based on the meteorological conditions, and the relationship would be more positive in hot and dry environment as compared to hot and humid environment.

The increase in soil water content with increase in temperature can be explained by a two-step process whereby increased soil temperature leads to loss of surface soil moisture and that in turn causes the movement of water in the form of vapor from the subsoil to the surface soil layers due to the available temperature gradient. The 80 non-rainfall days were mainly considered in order to evaluate if this relationship was valid under both rainfall and without rainfall scenarios, with the assumption that without rainfall there will not be enough water source to increase the soil water content. The only source could have been either fog or the soil moisture and groundwater present in the subsoil. However, since fog events generally occur at lower temperature and during early morning hours, this reasoning favorably points towards the available soil moisture and groundwater. Henceforth, this relationship suggests that the increase in the soil water content may be due to the water vapor transport from the soil moisture and the groundwater available at few meters below the soil surface.

4.2 Modeled water vapor surface fluxes

The use of HYDRUS-1D model for the simulation of actual surface flux is to examine if the process of water vapor transport in the subsoil will lead to some contribution in the fog formation (Figure 8). The low value of R^2 for the soil water content may be due to the approximation of the soil hydraulic parameters and the heat transport parameters required during the simulation process. Due to the lack of actual field-measured soil hydraulic parameters such as saturated water content and saturated hydraulic conductivity, the Rosetta Lite v.1.1 that is available in HYDRUS-1D model was used to predict the values of these parameters. The residual water content was also predicted by the Rosetta, and was higher than the initial water content observed in the field. However, since HYDRUS-1D model requires the residual water content to be lower than the initial water content to initiate the model run, the residual water content had to be manually attuned and hence a value lower than the initial water content was assigned. The constraints of field measured soil hydraulic parameters may be one of the reasons for the simulated soil water content not being quite synchronized with the observed values.

The thermal conductivity equation and heat transport parameters used in this study are the ones provided by Chung and Horton (1987). The HYDRUS-1D model has the option to choose the thermal conductivity values from either sand, clay or loam options. Because the sites considered in this study are mostly sandy, the heat transport parameters for sand as provided by the model are applied. Further, since temperature at lower boundary was not available in the daily temporal resolution, a constant temperature of 25°C was assumed at the gravel plains because this was the temperature measured at the site near the groundwater depth, and a constant temperature of 24°C was assumed at the sand dunes since the soil temperature at the sand dunes was found lower than at the gravel plains (for temperature profile modeled by HYDRUS-1D, see Figure 3 in

Supplementary materials). This assumption of constant temperature at the lower boundaries may also be a reason for the differences between the modeled and observed water content values. As indicated from previous literature, soil temperature at around 100 cm depth would remain within a range of few degrees (approximately 0.5 - 5°C) in the Namib Desert and locations with similar climatic conditions (Goudie, 1970; Lancaster et al., 1984; Kohler, 2010; Nicholson, 2011). For example, Goudie (1970) and Lancaster et al. (1984) presented soil temperature variation (from surface to 120 cm depth) in the Namib Desert. Kohler (2010) showed the soil temperature variation from soil surface to 100 cm depth in Western Africa, and Nicholson (2011) compiled soil temperature from surface to 75 cm depth over a sand dune in the Sahara based on the work of Peel (1974). Additional model runs were performed to simulate surface flux using temperature ranging from 20 to 30°C for both study sites. The results showed that temperature changes did not alter the values of heat flux drastically at both sites (see Figure 4, Supplementary materials).

The validation period was selected after excluding approximately 40% of the overall simulation period in the beginning to make sure that the model reached a stable state. Although in a different way from precipitation, fog also increases the soil water content (Li et al., 2018), but the HYDRUS-1D model does not have a direct option to address any non-rainfall events such as fog. Since the fog was not assigned into the model, the possibility of soil moisture recharge by the fog water was not considered by the model. This may have caused simulated water content values to be lower than the field observed ones (Figure 6). In addition, water uptake by plants roots was neglected in this study since vegetation cover near the study sites was extremely low. Despite the low abundance of vegetation, if water uptake by plant roots were considered, the soil moisture and actual surface flux probably might have been higher since the presence of a vegetation cover is

supposed to increase the soil water content as compared to the bare ground conditions that currently prevail at the study sites (Li et al., 2016).

The minimum pressure head at the soil surface (h_{CritA} , a variable in HYDRUS-1D) was required by the HYDRUS-1D model when the atmospheric boundary condition was selected at the upper boundary, and was set to 10^{-5} cm (for pressure head profile modeled by HYDRUS-1D, see Figure 5 in Supplementary materials). Additional model runs were included by varying the minimum pressure head values to check if there were significant changes in the surface flux values (see Figure 6 in Supplementary materials). The results showed that even though there was a small change in the magnitude of flux obtained, the resulting flux mostly matches the polarity in reported values (positive and negative). The actual surface flux at both sites exhibits similar patterns but different magnitudes (Figure 8), and this may be due to the similar meteorological conditions shared by the sites. It is also evident that the actual surface water vapor flux obtained from the model is lower at the sand dunes site as compared to the gravel plains. This may be attributed to the difference in soil texture at the sites.

The actual surface flux and evaporation values as obtained from the HYDRUS-1D model clearly depicts that there is water vapor exchange throughout the period from the soil to the atmosphere, and this could contribute to the formation of radiation fog as well as mixed fog in the area. The positive flux of water vapor at the soil surface suggest a constant transfer of soil water near the surface to the atmosphere, and over time this cumulated water vapor under favorable meteorological conditions may lead to the formation of fog.

5. Conclusions

Soil moisture can be a potential source of fog in dryland ecosystems like the Namib Desert. The field observation analysis showed that there was an increase in volumetric soil water content

near soil surface with increase in soil or air temperature, which is a new finding, and an important piece of evidence of the biophysical basis of water vapor movement. The relationship was similar during the entire study period as well as for a rainless period of 80 days. The study results documented the transfer of water vapor in amount sufficient to support the formation of fog at the study sites selected for this research. Field observations supported by the results of hydrological modeling have demonstrated the possible contribution of soil moisture to fog formation through water vapor movement. This research has for the first time demonstrated the possibility for subsoil water (soil moisture) to participate in the formation of fog, specifically radiation fog in the Namib Desert. The modeling results suggest that this approach can be further utilized to study possible fog sources in other regions.

Acknowledgments

The authors declare no financial conflicts or interests. Funding for this work was made available from the U.S. National Science Foundation (IIA-1427642 and CAREER award EAR-1554894). We would like to acknowledge Gobabeb Research and Training Centre for access to the FogNet weather stations and for the logistical support and fieldwork assistance. We thank two anonymous reviewers for their constructive comments, which significantly improved the quality of this manuscript.

References

- Adeel, Z., U. Safriel, D. Niemeijer and R. White (2005). Ecosystems and human well-being: desertification synthesis, World Resources Institute (WRI).
- Bergot, T. and D. Guedalia (1994). Numerical forecasting of radiation fog. Part I: Numerical model and sensitivity tests. *Monthly Weather Review* 122(6): 1218-1230.

- Bittelli, M., F. Ventura, G. S. Campbell, R. L. Snyder, F. Gallegati and P. R. Pisa (2008). Coupling of heat, water vapor, and liquid water fluxes to compute evaporation in bare soils. *Journal of Hydrology* 362(3): 191-205.
- Cahill, A. T. and M. B. Parlange (1998). On water vapor transport in field soils. *Water Resources Research* 34(4): 731-739.
- Chung, S. O. and R. Horton (1987). Soil heat and water flow with a partial surface mulch. *Water Resources Research* 23(12): 2175-2186.
- D'Odorico, P. and A. Porporato (2006). In *Dryland Ecohydrology* (pp. 31-46). Springer, Dordrecht.
- Dawson, T. E. (1998). Fog in the California redwood forest: ecosystem inputs and use by plants. *Oecologia* 117(4): 476-485.
- Eckardt, F., K. Soderberg, L. Coop, A. Muller, K. Vickery, R. Grandin, C. Jack, T. Kapalanga and J. Henschel (2013). The nature of moisture at Gobabeb, in the central Namib Desert. *Journal of Arid Environments* 93: 7-19.
- Eltahir, E. A. (1998). A soil moisture–rainfall feedback mechanism: 1. Theory and observations. *Water Resources Research* 34(4): 765-776.
- Entekhabi, D., J. L. Privette and J. A. Berry (2001). Assessing the relationship between surface temperature and soil moisture in southern Africa. *Remote Sensing and Hydrology 2000: A Selection of Papers Presented at the Conference on Remote Sensing and Hydrology 2000, Held at Santa Fe, New Mexico, USA, April 2000, International Assn of Hydrological Sciences*.
- Eugster, W. (2008). Fog research. *Die Erde* 139(1-2): 1-10.

- Fang, X., Zhao, W., Wang, L., Feng, Q., Ding, J., Liu, Y., & Zhang, X. (2016). Variations of deep soil moisture under different vegetation types and influencing factors in a watershed of the Loess Plateau, China. *Hydrol. Earth Syst. Sci.*, 20, 3309-3323.
- Goudie, A. (1970). Climate, weathering, crust formation, dunes, and fluvial features of the Central Namib Desert, near Gobabeb, South West Africa. *Madoqua*, 2(1), 15-31.
- Ingraham, N. L., & Matthews, R. A. (1988). Fog drip as a source of groundwater recharge in northern Kenya. *Water Resources Research*, 24(8), 1406-1410.
- Ingraham, N. L., & Matthews, R. A. (1990). A stable isotopic study of fog: the Point Reyes Peninsula, California, USA. *Chemical Geology: Isotope Geoscience section*, 80(4), 281-290.
- Kaseke, K. F., L. Wang and M. K. Seely (2017). Nonrainfall water origins and formation mechanisms. *Science Advances* 3(3): e1603131.
- Kaseke, K. F., L. Wang, H. Wanke, C. Tian, M. Lanning and W. Jiao (2018). Precipitation origins and key drivers of precipitation isotope (^{18}O , ^2H , and ^{17}O) compositions over windhoek. *Journal of Geophysical Research: Atmospheres* 123(14): 7311-7330.
- Kaseke, K. F., Tian, C., Wang, L., Seely, M., Vogt, R., Wassenaar, T., & Mushi, R. (2018). Fog spatial distributions over the Central Namib Desert-an isotope approach. *Aerosol and Air Quality Research*, 18, 49-61.
- Kohler, M., Kalthoff, N., & Kottmeier, C. (2010). The impact of soil moisture modifications on CBL characteristics in West Africa: A case-study from the AMMA campaign. *Quarterly Journal of the Royal Meteorological Society*, 136(S1), 442-455.
- Lancaster, J., Lancaster, N., & Seely, M. K. (1984). Climate of the central Namib Desert. *Madoqua*, 14(1), 5-61.

- Li, B., L. Wang, K. F. Kaseke, L. Li and M. K. Seely (2016). The impact of rainfall on soil moisture dynamics in a foggy desert. *PloS one* 11(10): e0164982.
- Li, B., L. Wang, K. F. Kaseke, R. Vogt, L. Li and M. K. Seely (2018). The impact of fog on soil moisture dynamics in the Namib Desert. *Advances in Water Resources* 113: 23-29.
- Liu, W. J., Zhang, Y. P., Li, H. M., & Liu, Y. H. (2005). Fog drip and its relation to groundwater in the tropical seasonal rain forest of Xishuangbanna, Southwest China: a preliminary study. *Water Research*, 39(5), 787-794.
- Lu, X., Wang, L., Pan, M., Kaseke, K. F., & Li, B. (2016). A multi-scale analysis of Namibian rainfall over the recent decade—comparing TMPA satellite estimates and ground observations. *Journal of Hydrology: Regional Studies*, 8, 59-68.
- Miller, G.R., Cable, J.M., McDonald, A.K., Bond, B., Franz, T.E., Wang, L., Gou, S., Tyler, A.P., Zou, C.B. & Scott, R.L. (2012). Understanding ecohydrological connectivity in savannas: a system dynamics modelling approach. *Ecohydrology*, 5(2), 200-220.
- Nicholson, S. E. (2011). *Dryland climatology*. Cambridge University Press.
- Peel, R. F. (1974). Insolation weathering: some measurements of diurnal temperature changes in exposed rocks in the Tibesti region, central Sahara, *Zeitschrift für Geomorphologie, Supp.*, 21, 19-28. Schweizerbart Publishers, www.schweizerbart.de.
- Prada, S., Cruz, J. V., Silva, M. O., & Figueira, C. (2010). Contribution of cloud water to the groundwater recharge in Madeira Island: preliminary isotopic data. In *Proceedings of the Fifth International Conference on Fog, Fog Collection and Dew* (pp. 25-30). Münster,, Germany: Copernicus Meetings and University of Münster, Institute for Landscape Ecology Climatology.

- Qiao, N., Zhang, L., Huang, C., Jiao, W., Maggs-Kölling, G., Marais, E., & Wang, L. (2020). Satellite observed positive impacts of fog on vegetation. *Geophysical Research Letters*, 47, e2020GL088428. <https://doi.org/10.1029/2020GL088428>
- Runyan, C., Wang, L., Lawrence, D., & D'Odorico, P. (2019). Ecohydrological Controls on the Deposition of Non-rainfall Water, N, and P to Dryland Ecosystems. In *Dryland Ecohydrology* (pp. 121-137). Springer, Cham.
- Saito, H., J. Šimůnek and B. P. Mohanty (2006). Numerical analysis of coupled water, vapor, and heat transport in the vadose zone. *Vadose Zone Journal* 5(2): 784-800.
- Sakai, M., S. B. Jones and M. Tuller (2011). Numerical evaluation of subsurface soil water evaporation derived from sensible heat balance. *Water Resources Research* 47(2).
- Sawaske, S. R., & Freyberg, D. L. (2015). Fog, fog drip, and streamflow in the Santa Cruz Mountains of the California Coast Range. *Ecohydrology*, 8(4), 695-713.
- Schaap, M. G., F. J. Leij and M. T. Van Genuchten (2001). Rosetta: A computer program for estimating soil hydraulic parameters with hierarchical pedotransfer functions. *Journal of Hydrology* 251(3-4): 163-176.
- Šimůnek, J., M. Šejna, H. Saito, M. Sakai and M. T. Van Genuchten (2013). The HYDRUS-1D Software Package for Simulating the One-Dimensional Movement of Water, Heat, and Multiple Solutes in Variably-Saturated Media, Version 4: 281.
- Van Genuchten, M. T. (1980). A closed-form equation for predicting the hydraulic conductivity of unsaturated soils 1. *Soil science society of America journal* 44(5): 892-898.
- Wang, L., D'Odorico, P., Manzoni, S., Porporato, A., & Macko, S. (2009). Carbon and nitrogen dynamics in southern African savannas: the effect of vegetation-induced patch-scale heterogeneities and large scale rainfall gradients. *Climatic Change*, 94, 63-76.

- Wang, L., D'Odorico, P., Ries, L., Caylor, K., & Macko, S. (2010). Combined effects of soil moisture and nitrogen availability variations on grass productivity in African savannas. *Plant and Soil*, 328, 95-108, 110.1007/s11104-11009-10085-z.
- Wang, L., P. D'Odorico, J. Evans, D. Eldridge, M. McCabe, K. Caylor and E. King (2012). Dryland ecohydrology and climate change: critical issues and technical advances. *Hydrology and Earth System Sciences* 16(8): 2585-2603.
- Wang, L., K. F. Kaseke and M. K. Seely (2017). Effects of non-rainfall water inputs on ecosystem functions. *Wiley Interdisciplinary Reviews: Water* 4(1): e1179.
- Wang, L., Kaseke, K. F., Ravi, S., Jiao, W., Mushi, R., Shuuya, T., & Maggs-Kölling, G. (2019). Convergent vegetation fog and dew water use in the Namib Desert. *Ecohydrology*, 12, e2130.
- Wei, F., Wang, S., Fu, B., Wang, L., Liu, Y. Y., & Li, Y. (2019). African dryland ecosystem changes controlled by soil water. *Land Degradation & Development*, 30, 1564-1573.
- Yin, J., D'Odorico, P., & Porporato, A. (2019). Soil Moisture Dynamics in Water-Limited Ecosystems. In *Dryland Ecohydrology* (pp. 31-48). Springer, Cham.
- Yu, K., & D'Odorico, P. (2015). Hydraulic lift as a determinant of tree–grass coexistence on savannas. *New Phytologist*, 207(4), 1038-1051.

TABLES

Table 1. Soil hydraulic parameters used in the HYDRUS-1D model for two sites: sand dunes and gravel plains.

Soil Hydraulic Parameters	Sand dunes	Gravel plains
Residual water content, Q_r [-]	0.001	0.01
Saturated water content, Q_s [-]	0.3886	0.3865
Parameter alpha [1/cm]	0.034	0.038
Parameter n [-]	1.558	3.35
Saturated hydraulic conductivity, K_s [cm/days]	70.01	428.95
Parameter, l [-]	0.5	0.5

Table 2. Heat transport parameters used in the HYDRUS-1D model for two sites: sand dunes and gravel plains.

Heat transport parameters	Sand dunes	Gravel plains
Volume fraction of solid phase	0.6114	0.6135
Volume fraction of organic matter	0	0
Longitudinal thermal dispersivity	5	5
Coefficient b1 for thermal conductivity function	1.47E+16	1.47E+16
Coefficient b2 for thermal conductivity function	-1.55E+17	-1.55E+17
Coefficient b3 for thermal conductivity function	3.17E+17	3.17E+17
Volumetric heat capacity of solid phase (Cn)	1.43E+14	1.43E+14
Volumetric heat capacity of organic matter (Co)	1.87E+14	1.87E+14
Volumetric heat capacity of liquid phase (Cw)	3.12E+14	3.12E+14

Table 3. Descriptive and correlation statistics (with soil temperature) of volumetric water content from field observations for the overall study period and the 80 non-rainfall days at sand dunes and gravel plains.

Statistics	Overall study period		80 non-rainfall days (Aug.19 – Nov. 6, 2015)	
	Sand dunes	Gravel plains	Sand dunes	Gravel plains
Mean (%)	0.771	2.105	0.639	1.499
Std. Dev. (%)	0.52	1.24	0.05	0.07
Kurtosis (k-value)	34.82	18.52	0.47	1.2
Skewness	4.95	3.9	-0.54	0.73
Spearman coefficient	0.50 ^{***}	0.27 _# ^{***}	0.67 ^{***}	0.28 _# [*]

* p-value < 0.05, *** p-value < 0.001,

Water content at lower soil temperatures (< 20°C) are removed since there may be some condensation effect.

Table 4. Statistics of volumetric water content (VMC), rainfall and fog for different hydrologic years at sand dunes and gravel plains.

Year	VWC_GP		VWC_SD		Rain (mm)				Fog (mm)			
	Mean	Std. Dev.	Mean	Std. Dev.	Rainfall days	Sum	Mean	Std. Dev.	Fog days	Sum	Mean	Std. Dev.
2013-2014*	0.018	0.002	N/A	N/A	2	1.6	0.006	0.071	N/A	N/A	N/A	N/A
2014-2015	0.020	0.011	0.006	0.001	4	14.1	0.039	0.468	63	142.62	0.493	0.011
2015-2016	0.019	0.010	0.007	0.002	2	21.7	0.059	1.065	76	174.30	0.480	0.010
2016-2017	0.020	0.011	0.006	0.003	4	11.8	0.032	0.406	45	81.46	0.288	0.011
2017-2018**	0.029	0.020	0.011	0.009	6	75.4	0.283	2.325	N/A	N/A	N/A	N/A

Note: VWC_GP = Volumetric water content at the gravel plains, VWC_SD = Volumetric water content at the sand dunes, Std. Dev. = Standard deviation, N/A = Not available
 *started from 12/29/2013, **ended on 6/24/2018
 Hydrologic year = October 1 to September 30

FIGURES

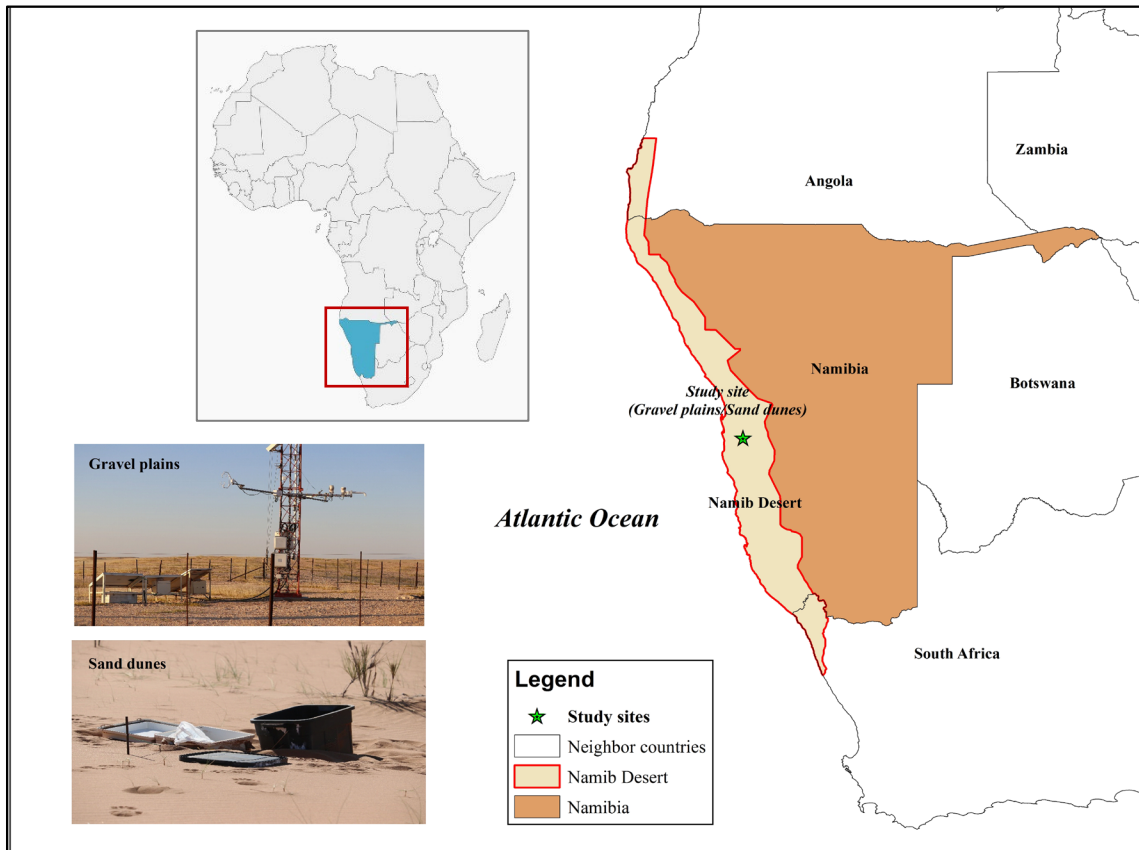


Figure 1. Extent of the Namib Desert and study site locations. The map shows the location of study sites, extent of Namib Desert, and two images taken at the site showing general characteristics of the study area.

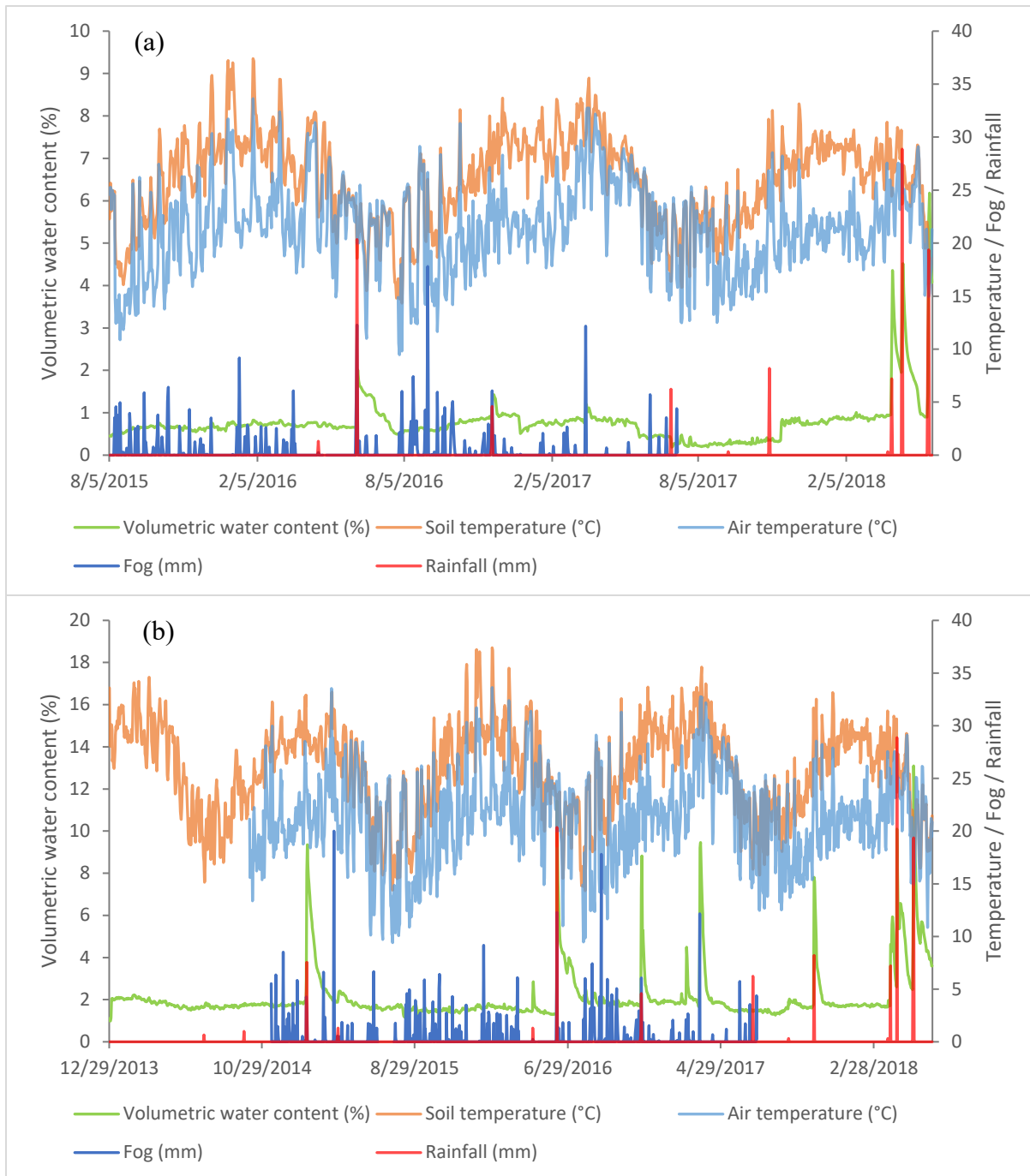


Figure 2. Variation of different variables (soil temperature (°C), air temperature (°C), volumetric water content (%), fog (mm) and rain (mm)) at the sand dunes from August 5, 2015 to May 22, 2018 (a) and at the gravel plains from December 29, 2013 to June 24, 2018 (b).

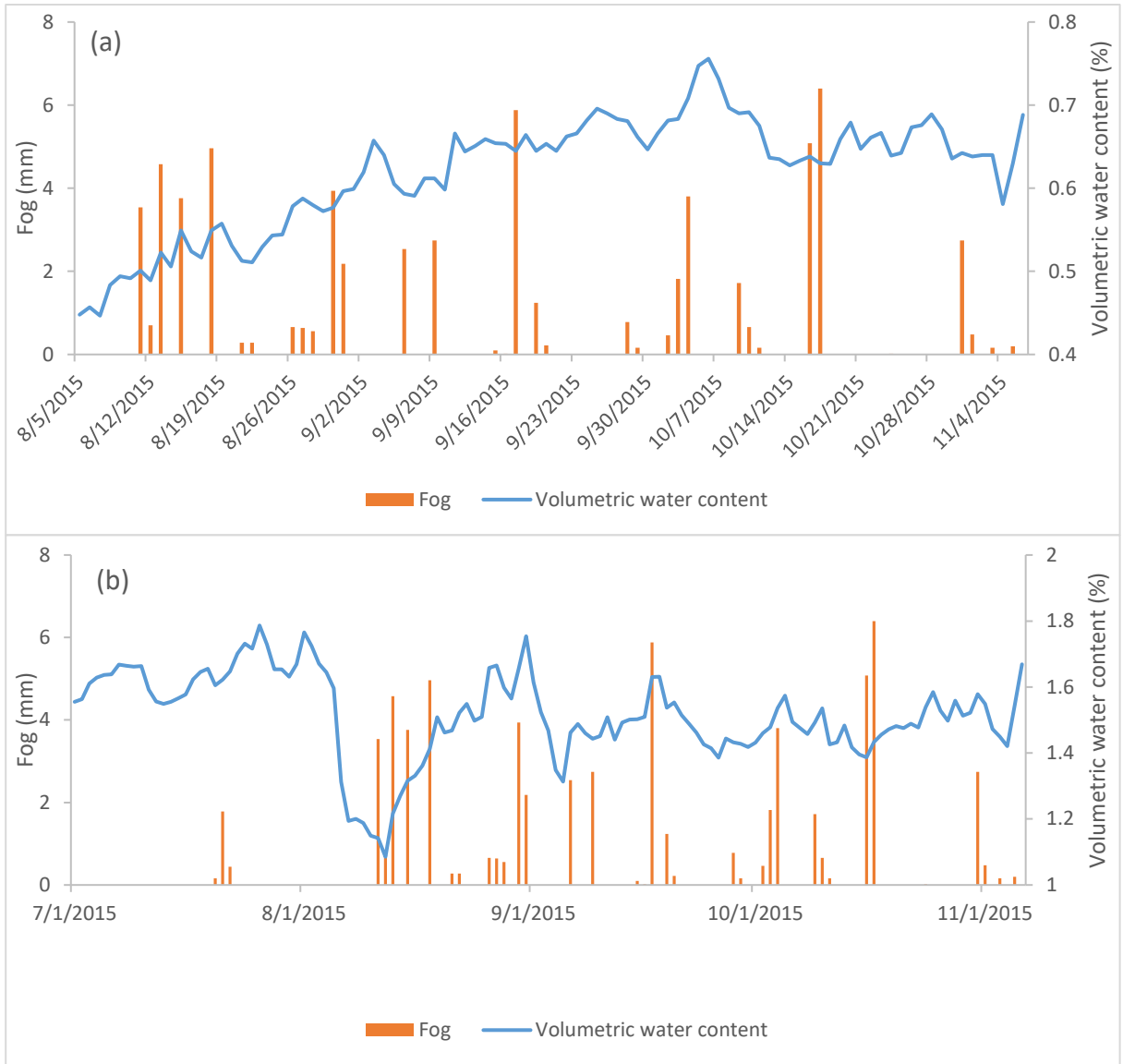


Figure 3. Fog (mm) and volumetric water content (%) at the sand dunes (a) and the gravel plains (b) during the modeling period.

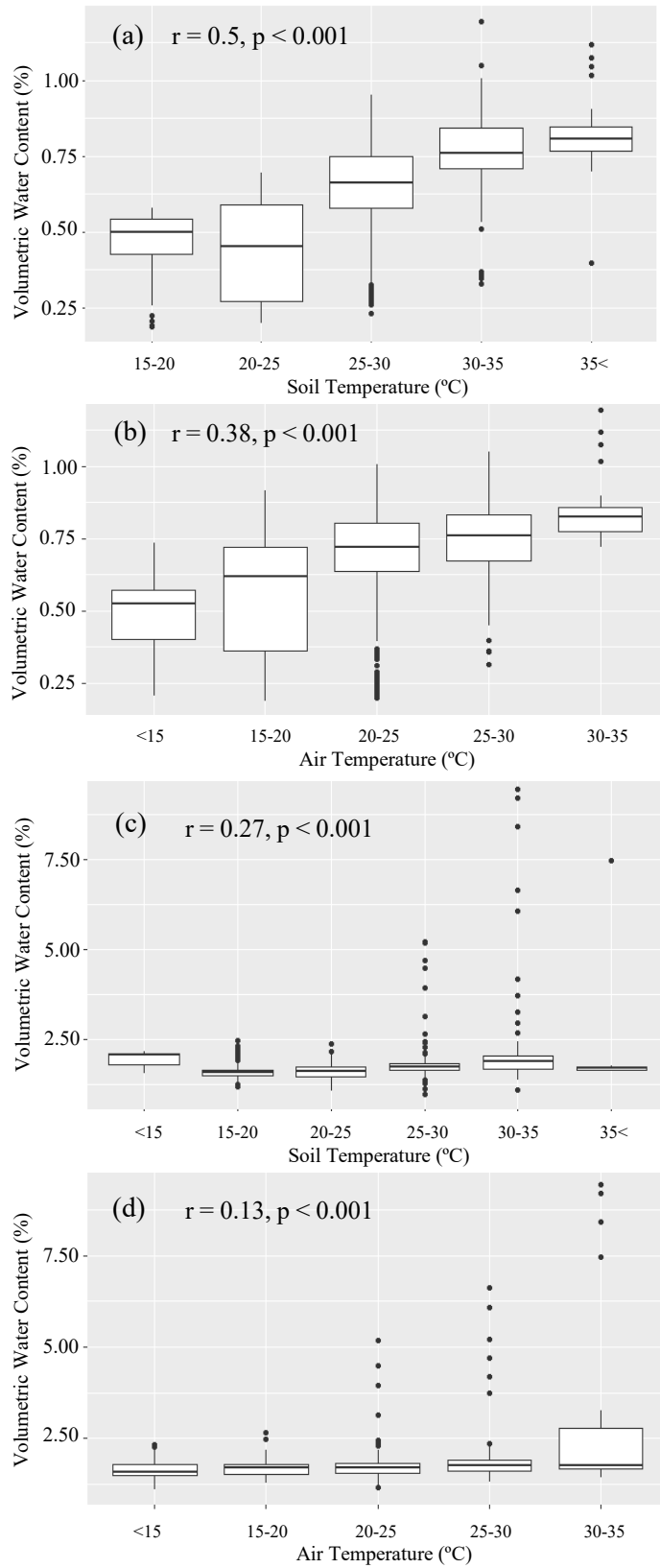


Figure 4. Relationship of volumetric water content with soil temperature and air temperature at the sand dunes (a, b) from August 5, 2015 to May 22, 2018 and the gravel plains (c, d) from December 29, 2013 to June 24, 2018.

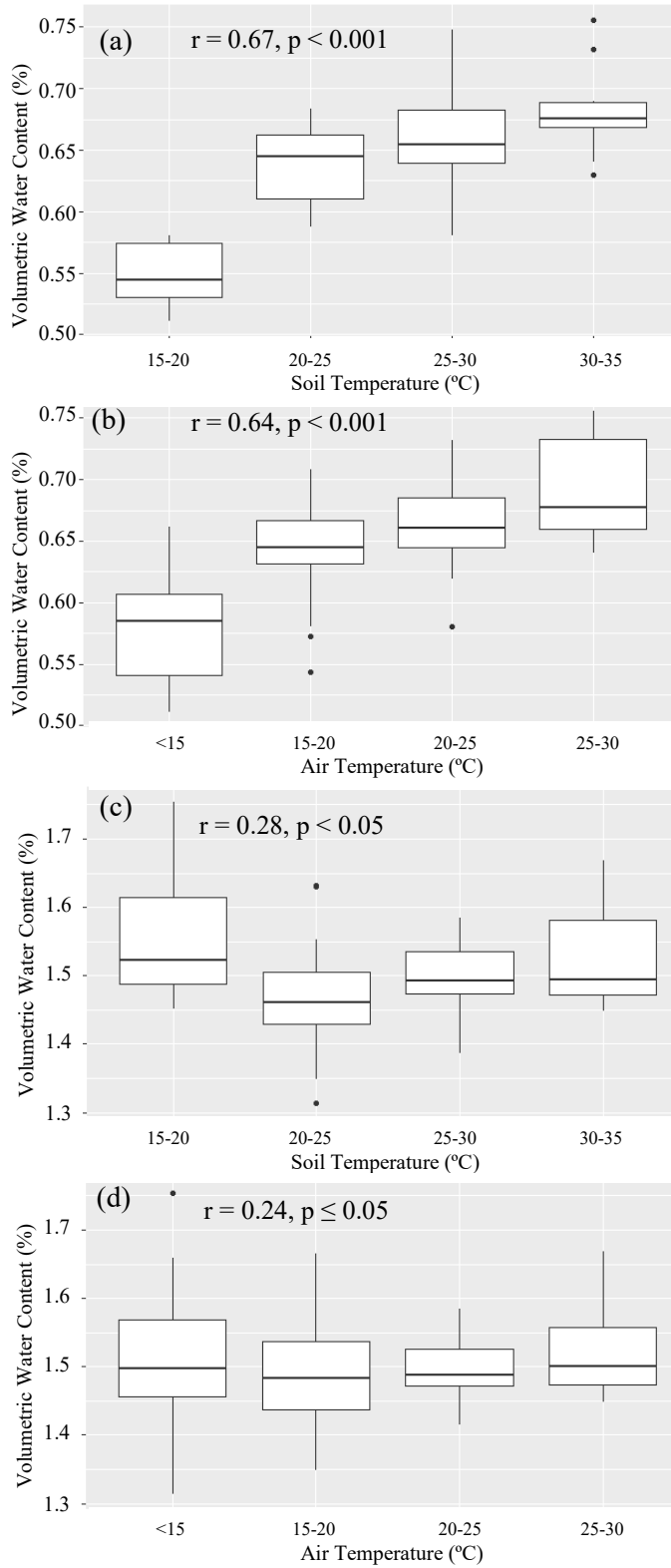


Figure 5. Relationship of volumetric water content with soil temperature and air temperature at the sand dunes (a, b) and the gravel plains (c, d) for 80 non-rainfall days from August 19, 2015 to November 6, 2015.

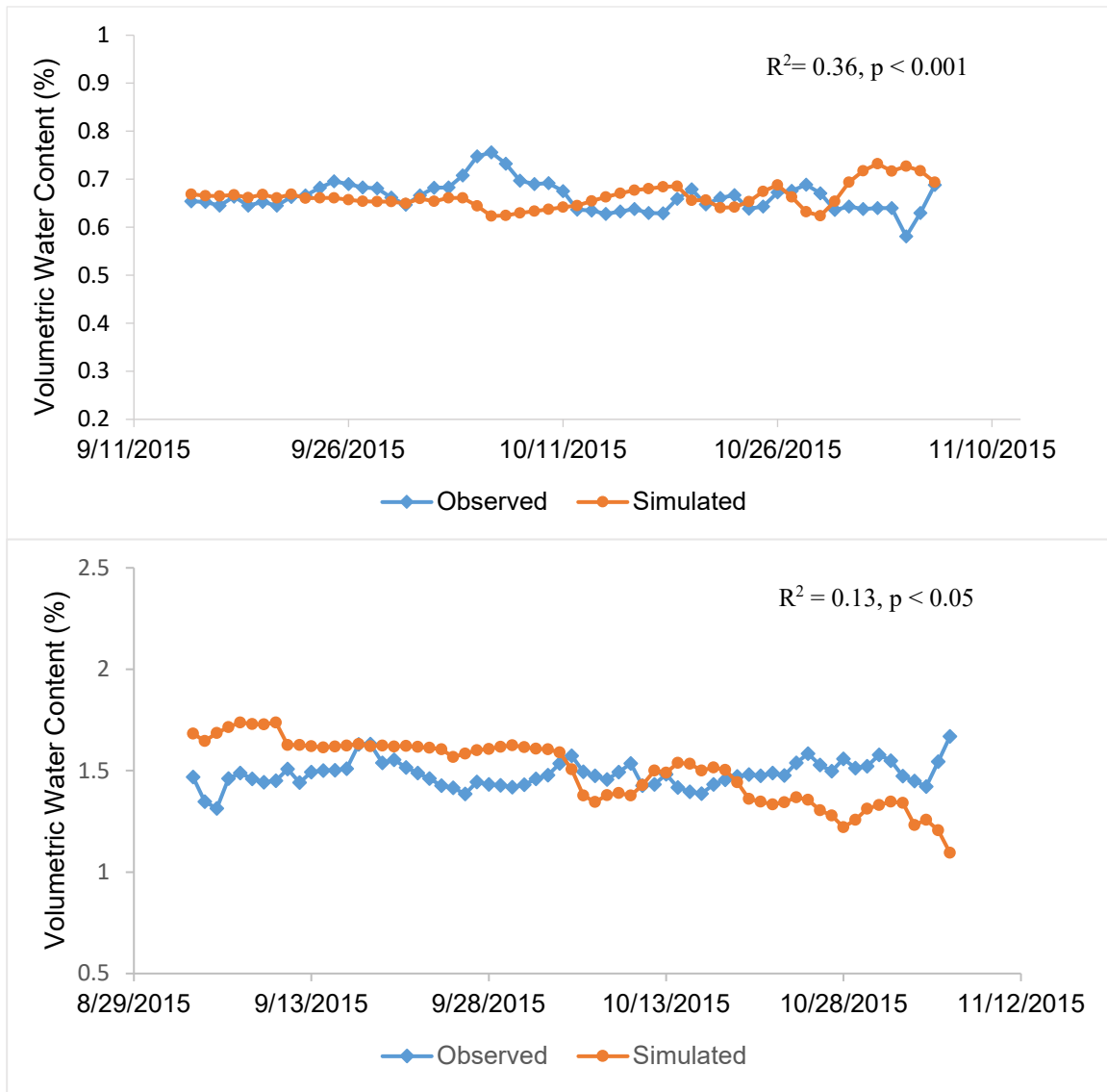


Figure 6. Observed and simulated volumetric water content at the sand dunes (a) and the gravel plains (b).

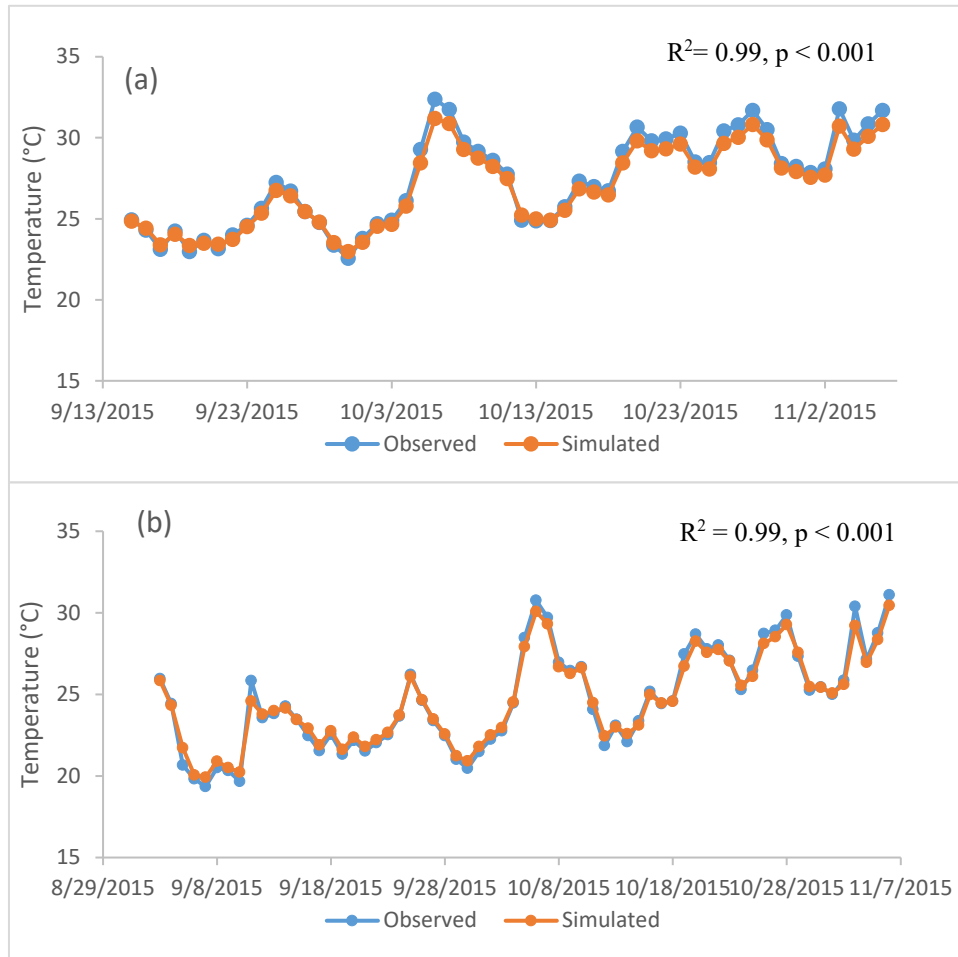


Figure 7. Observed and simulated soil temperature at the sand dunes (a) and the gravel plains (b).

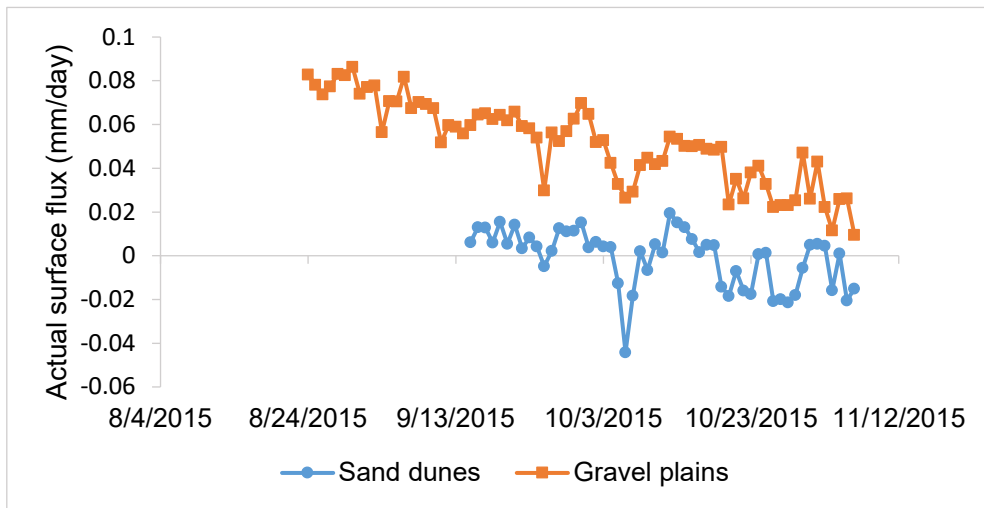


Figure 8. Surface flux (mm/day) obtained from HYDRUS-1D model at the sand dunes, and the gravel plains.

Supplementary materials

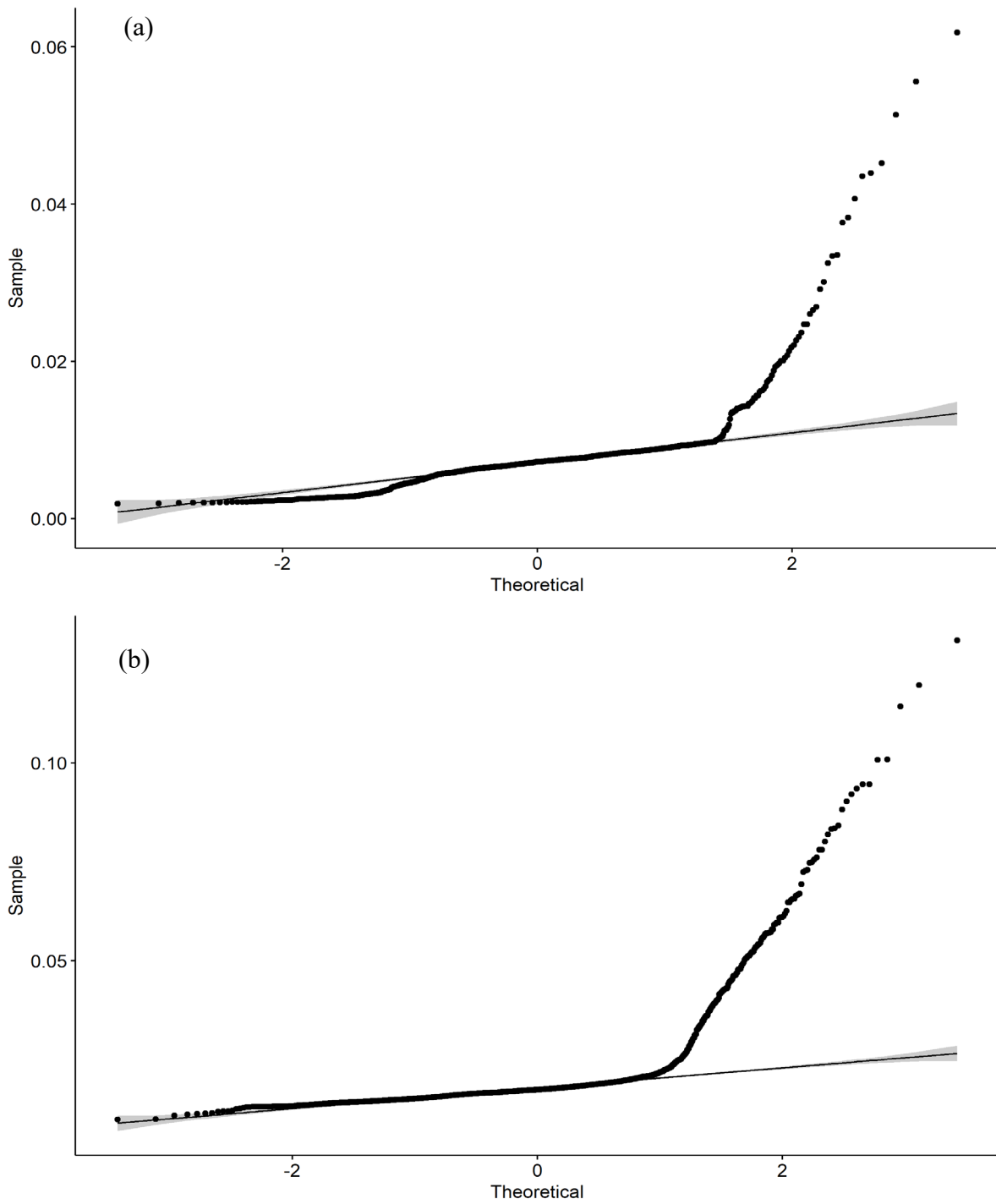


Figure 1. QQ-plot for the sand dunes (a) and the gravel plains (b) for the entire study period.

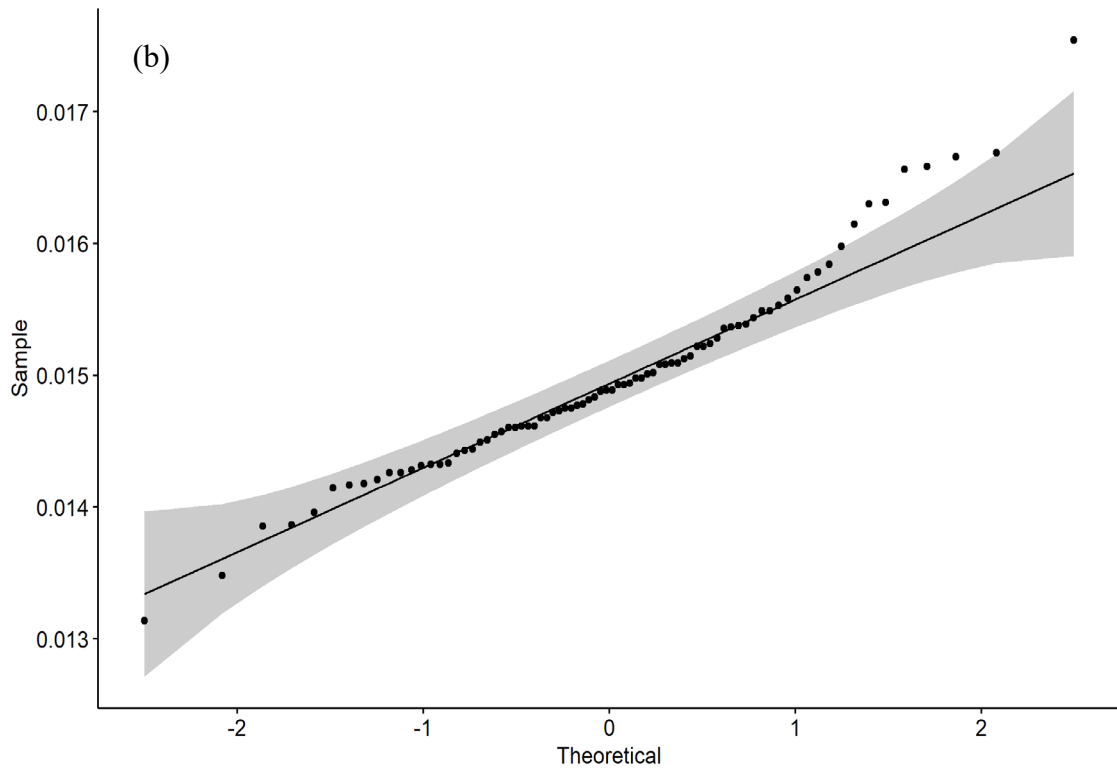
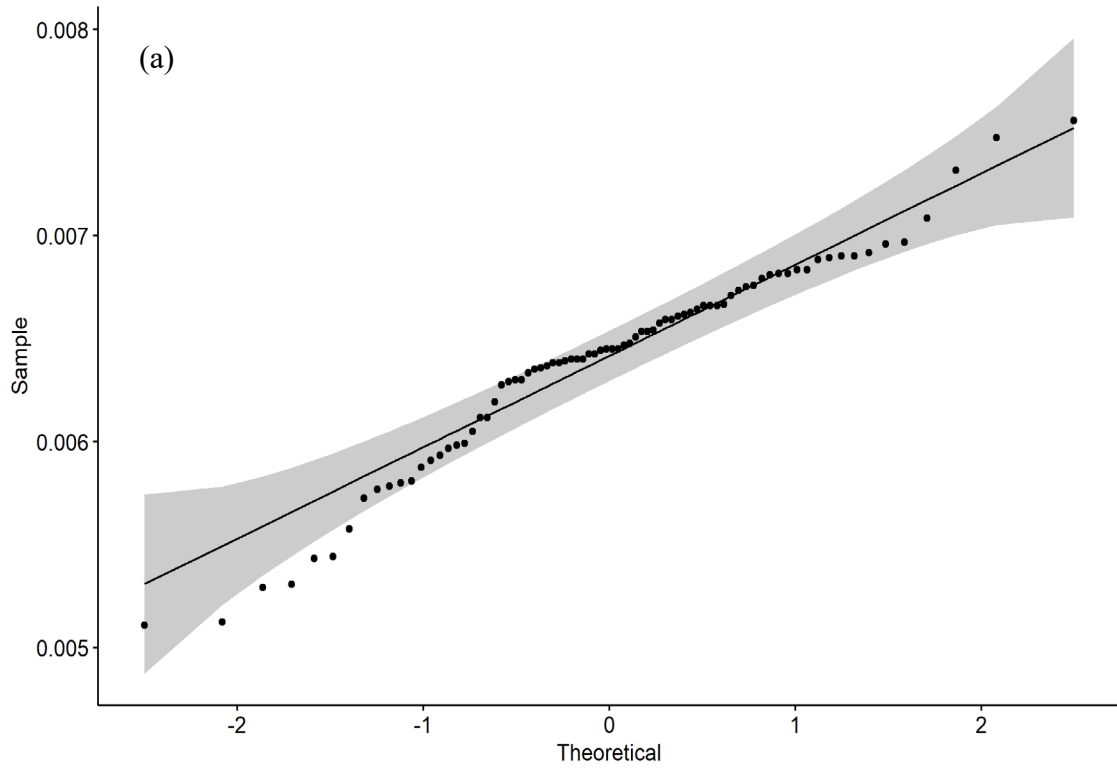


Figure 2. QQ-plot for the sand dunes (a) and the gravel plains (b) for the 80 non-rainfall days.

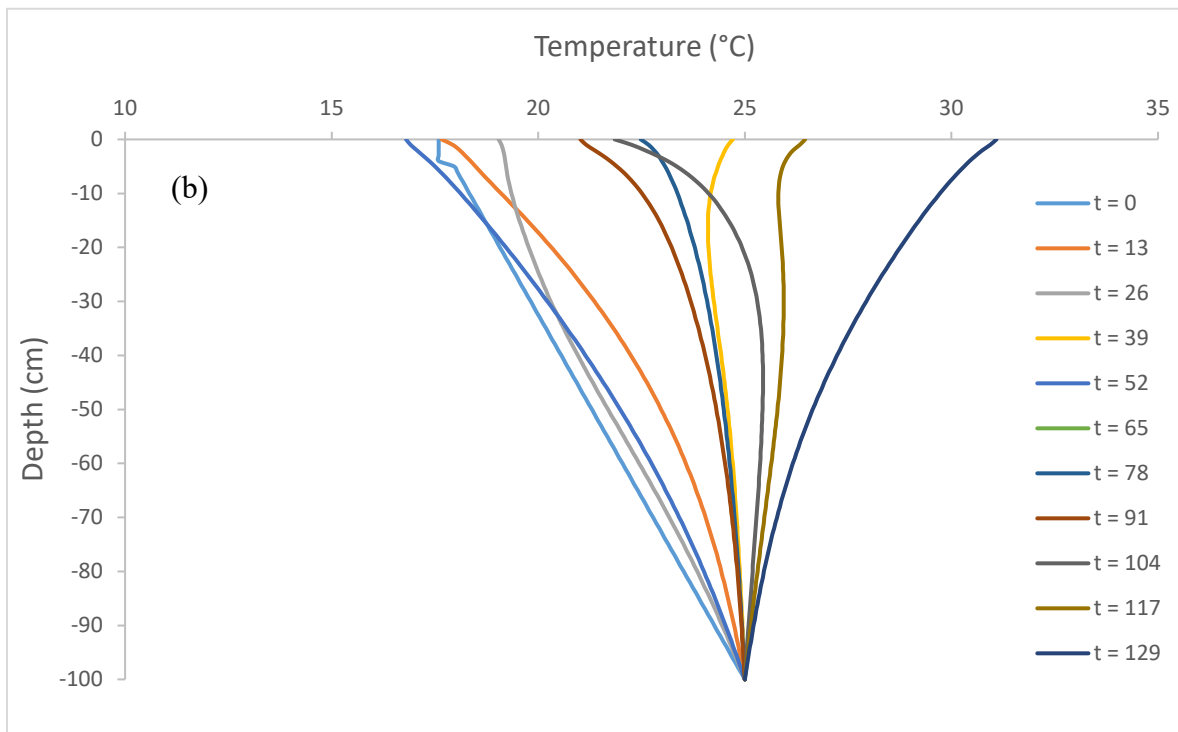
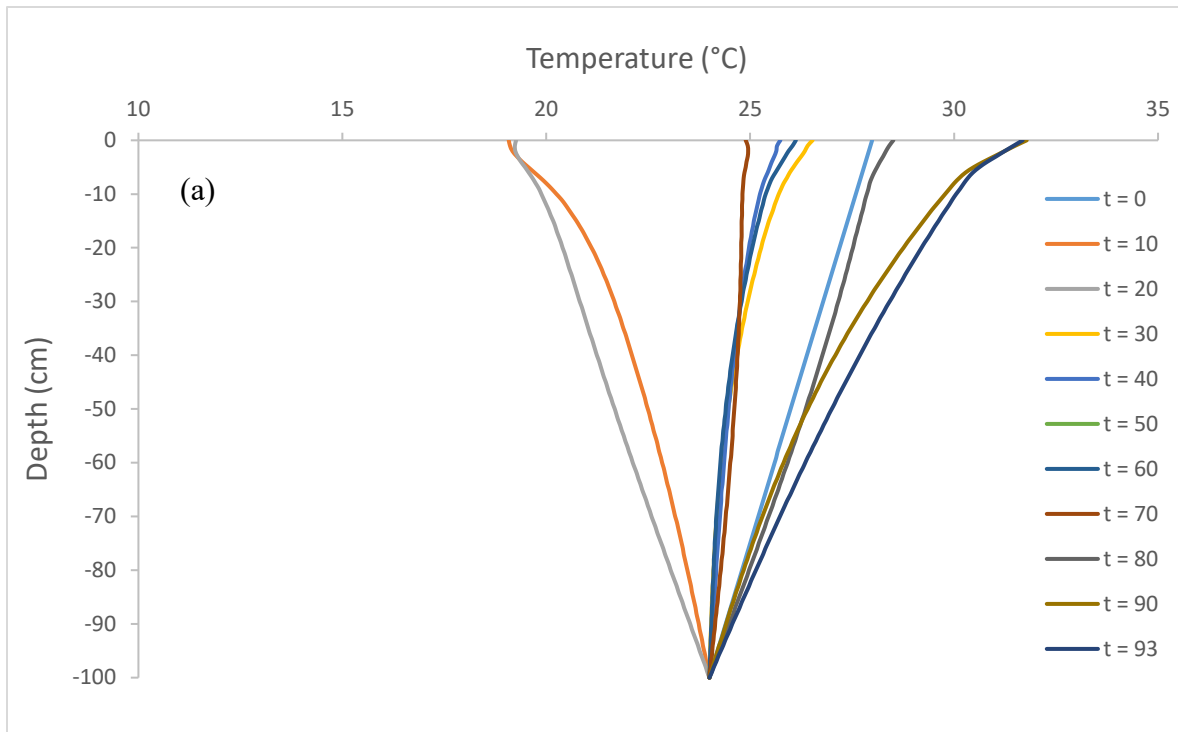


Figure 3. Soil temperature profiles modeled by HYDRUS-1D at different depths during the model run at the sand dunes (a) and the gravel plains (b). “t” in the legends represents the days at which the profiles are presented.

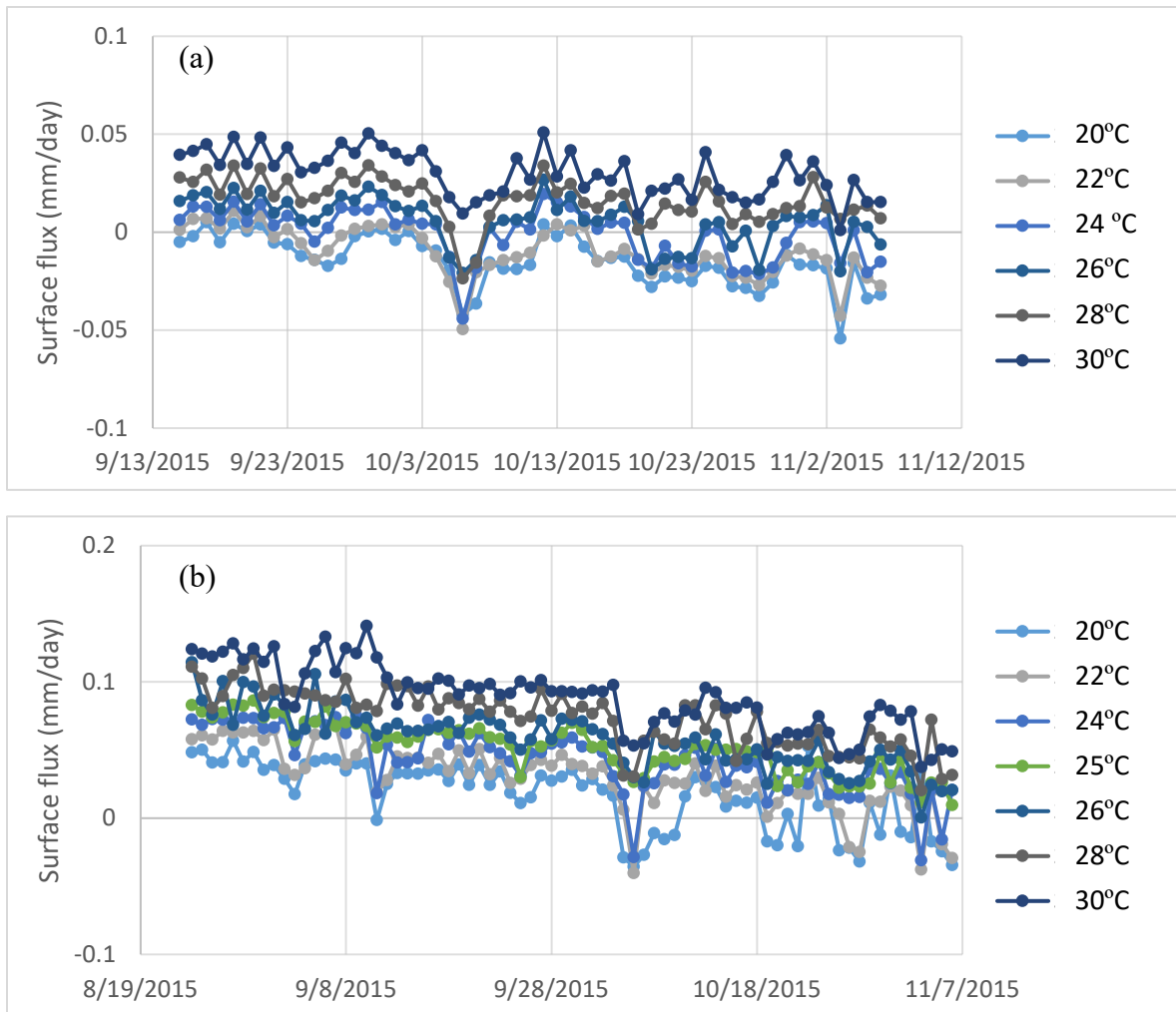


Figure 4. Surface flux at the sand dunes (a) and the gravel plains (b) with different lower boundary soil temperatures.

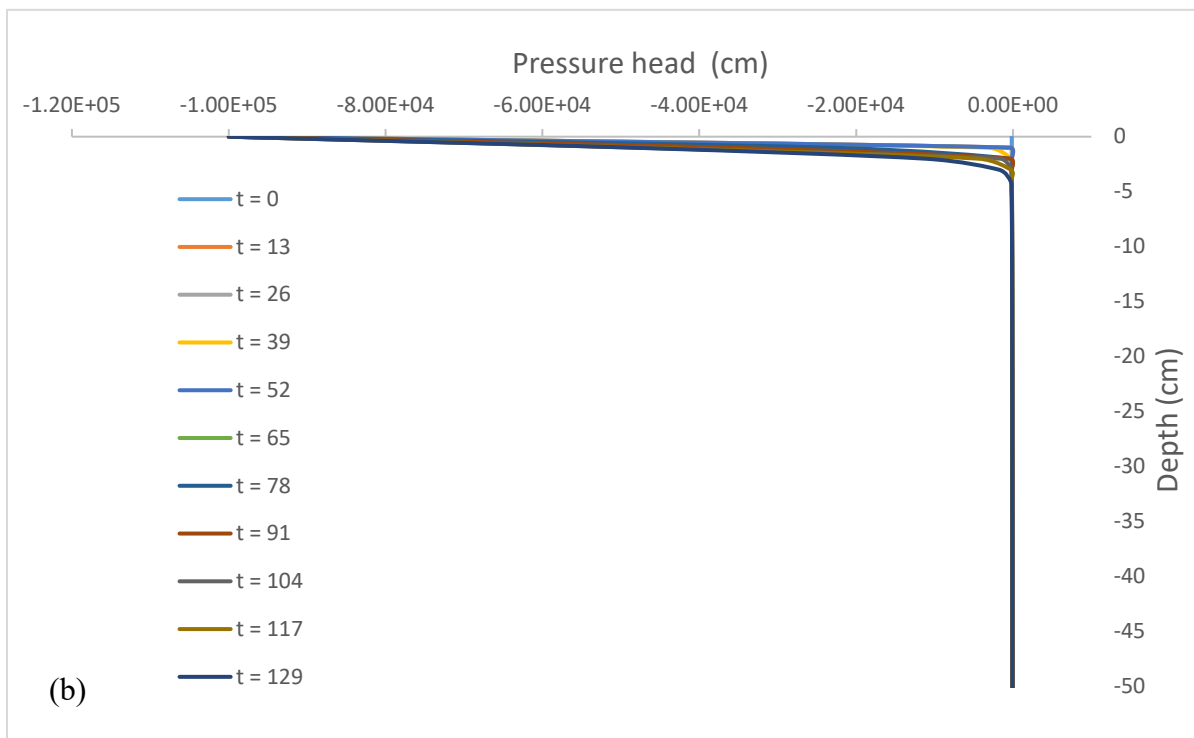
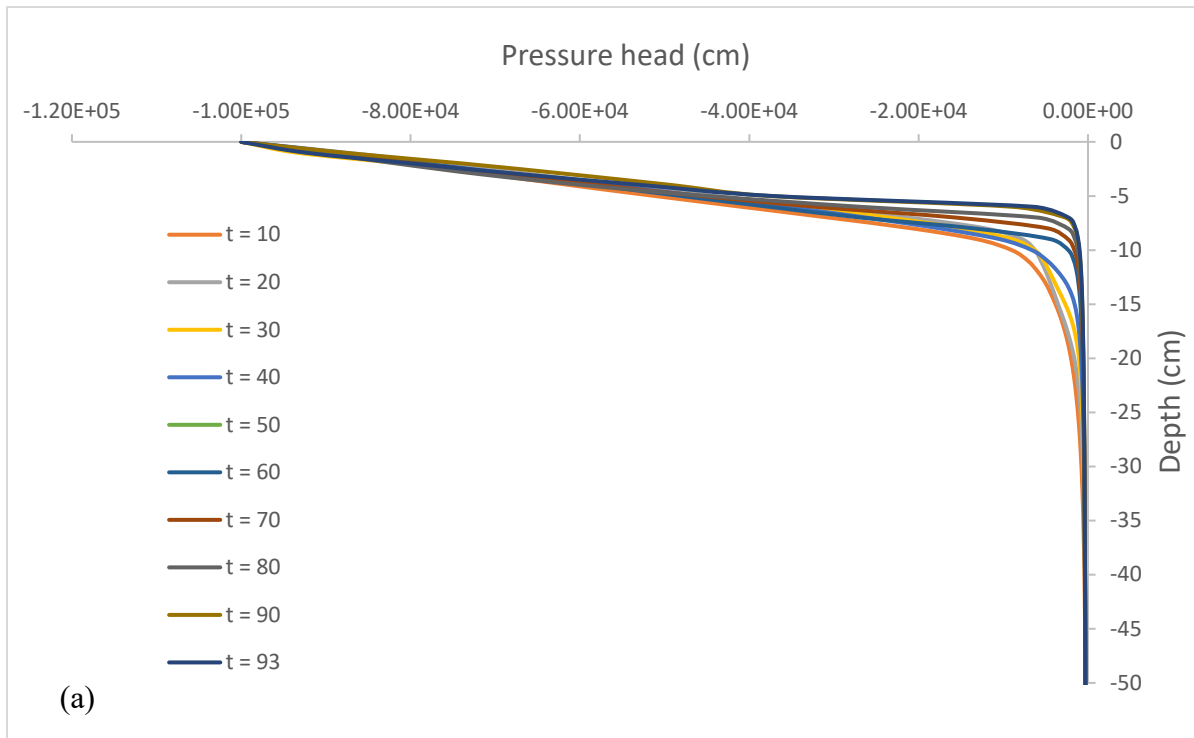


Figure 5. Pressure head profiles modeled by HYDRUS-1D at different depths during the model run at the sand dunes (a) and the gravel plains (b). “t” in the legends represents the days at which the profiles are presented.

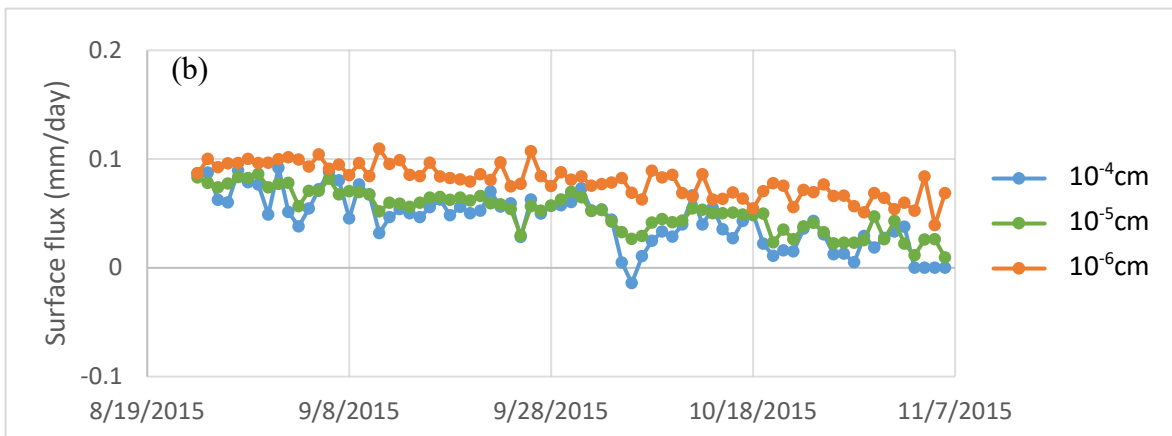
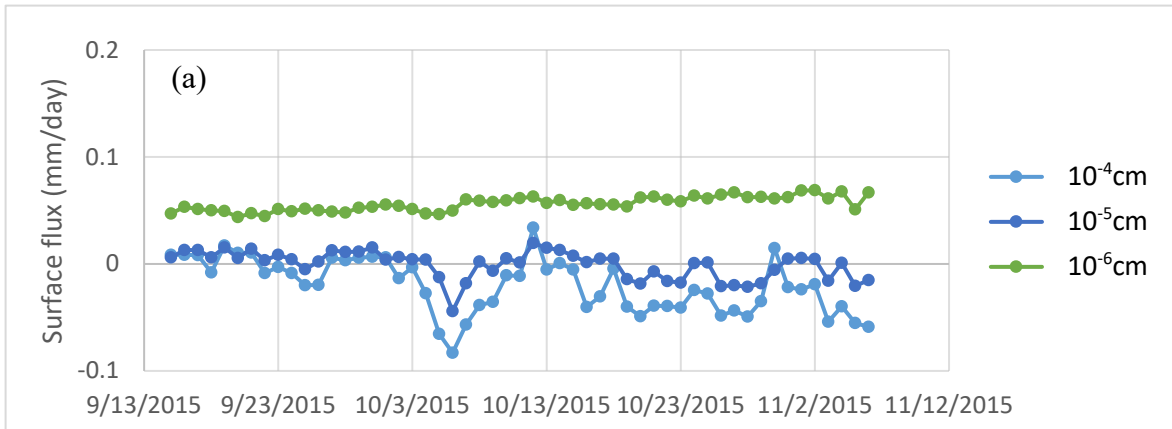


Figure 6. Surface flux at the sand dunes (a) and the gravel plains (b) with different minimum pressure head.